European Review for Medical and Pharmacological Sciences 2022; 26: 2875-2890

Radiological assessment of peritoneal carcinomatosis: a primer for resident

V. GRANATA[1], R. FUSCO[2], S. VENANZIO SETOLA[1], C. SASSAROLI[3], S. DE FRANCISCIS[3], P. DELRIO[3], G. DANTI[4,5], G. GRAZZINI[4,5], L. FAGGIONI[6], M. GABELLONI[6], A. OTTAIANO[7], S. GREGGI[8], R. PATRONE[9], R. PALAIA[9], A. PETRILLO[1], F. IZZO[9]

[1]Division of Radiology, "Istituto Nazionale Tumori IRCCS Fondazione Pascale – IRCCS di Napoli", Naples, Italy
[2]Medical Oncology Division, Igea SpA, Naples, Italy
[3]Division of Colorectal Surgery, Istituto Nazionale Tumori IRCCS Fondazione Pascale – IRCCS di Napoli, Naples, Italy
[4]Division of Radiology, "Azienda Ospedaliera Universitaria Careggi", Florence, Italy
[5]Italian Society of Medical and Interventional Radiology (SIRM), SIRM Foundation, Milan, Italy
[6]Department of Translational Research, University of Pisa, Pisa, Italy
[7]Abdominal Oncology Division, [8]Oncological Gynecology Division, [9]Division of Hepatobiliary Surgical Oncology, "Istituto Nazionale Tumori IRCCS Fondazione Pascale – IRCCS di Napoli", Naples, Italy

Abstract. **The imaging has critical responsibility in the assessment of peritoneal lesions along with estimating the overall extent. Valuing disease burden is crucial for selection of combining cytoreductive surgery (CRS) and intraperitoneal hyperthermic chemotherapy (HIPEC) treatment. An approach that combines the strength of several imaging tools and increases diagnostic accuracy, should be chosen, even if the preferred imaging tool in patients with suspected Peritoneal Carcinomatosis (PC) is CT.**

The outcomes of PC are mainly correlated to tumor spread, localization, and lesion size. Accurate assessment of these features is critical for prognosis and treatment planning. These data can be evaluated by Peritoneal Cancer Index (PCI), a quantitative index suggested by Harman and Sugarbaker. Additionally, precise predictive biomarkers should be established to predict PC in patients at risk. The radiomics analysis could predict PC throughout the evaluation of cancers heterogeneity.

Key Words:
Peritoneal carcinomatosis, Computed tomography, Magnetic resonance imaging, Diffusion weighted imaging, Peritoneal cancer index.

Introduction

Pathologic involvement of the peritoneum is due to a wide class of disorders, comprising as neoplastic as non-neoplastic disorders. Peritoneal carcinomatosis (PC) is the neoplastic involvement of peritoneal ligaments, mesenteries, and spaces[1-3]. Several gastrointestinal and gynaecological tumours could spread in the peritoneal space[4-10]. The presence of PC has been proven to drastically reduce overall survival (OS) in patients with gastrointestinal tumours[1]. It has been shown[1] that the 10%-35% of patients with recurrent colorectal cancer (CRC) and the 50% of patients with recurrent gastric cancer (GC), die due to PC complications. This outcome is appreciated in epithelial ovarian cancer (EOC) too[1]. However, while in PC due to OC, there is common agreement that peritoneal lesions eradication is correlated with longer survival, in CRC and GC complete PC eradication is frequently associated with short-term recurrence[1].

The recent knowledge of tumors biology, and the idea that peritoneum has a defensive role against cancer spreading, has fortified the concept that PC is a loco-regional disease, so that in absence of other systemic lesions, a multimodal approach, combining cytoreductive surgery (CRS), intraperitoneal hyperthermic chemotherapy (HIPEC) and systemic chemotherapy has been proposed[1,11-14]. In this scenario, the critical role of imaging is the identification of patients which could have advantage from this treatment, in order to avoid any unnecessary surgical treatments[15-20].

Peritoneal Dissemination and Others Route

PC is complicated series of events, known as the "peritoneal metastatic cascade". In the first phase,

Corresponding Author: Vincenza Granata, MD; e-mail: v.granata@istitutotumori.na.it

individual or clumps of cells break free of the primary lesion. They are then free to spread into the peritoneal cavity, with their final destination governed by many features, as gravity, movement of the abdominal viscera, flow of ascitic fluid, etc. Following peristaltic motion, cells enter into the peritoneal circulation and implant along the paracolic gutter, passing back up into the under-surface of the diaphragm. The first surface that free cells encounter is the mesothelium (the second step). The third step includes the infiltration of the mesothelial monolayer. The fourth step represents the invasion of the underlying connective tissue, that provides the necessary scaffold for tumor proliferation. The final step includes the angiogenesis to support tumor spread[21-25]. Other routes of propagation are: (*a*) the hematogenous, (*b*) contiguous and (*c*) lymphatic route. There are two main routes for lymphatic spreading, the lymphatic system of the greater omentum and the subphrenic lymphatic system. When the subphrenic lymphatic system becomes obstructed, ascites appears as a consequence[9].

Anatomy

The peritoneal cavity is the portion of the abdominal cavity delineated by the peritoneum, parietal and visceral peritoneum, and is a closed area. An open anatomic communication with the external area is only present in women through the genital organs [26-29]. Peritoneal ligaments are double layers or folds of peritoneum that support a structure within the peritoneal cavity; omentum and mesentery are precisely called peritoneal ligaments. Several abdominal ligaments develop from the ventral or dorsal mesentery[26]. They comprise the triangular ligament, the falciform ligament, the splenorenal ligament, the gastrosplenic ligament, the phrenic-colic ligament, the gastrocolic ligament, the greater omentum, the lesser omentum (formed by the gastrohepatic ligament and hepatoduodenal ligament), and the transverse mesocolon[26].

The transverse colon and mesocolon are the major landmarks separating the peritoneal cavity into supra-mesocolic and infra-mesocolic area. On the anterior side of the liver, the falciform ligament divide the supra-mesolic space is into the left and right subphrenic spaces. The right subphrenic space is situated under the right diaphragm and it extends caudally lateral to the liver to the right paracolic gutter, situated between the ascending colon and the lateral abdominal wall. The left subphrenic space is divided from the left paracolic gutter by the phrenic-colic ligament and the right subphrenic recess by the falciform ligament. This area comprises the gastrohepatic fossa, the gastrosplenic recess and the splenorenal recess. The splenorenal fossa continues anteriorly and medially behind the pancreas tail. The splenorenal fossa is in connexion with the left subphrenic space but it is divided from the lesser sac. Posteriorly, the falciform ligament is in continuity with the left and right triangular ligaments. The left triangular ligament is short and formed by the fusion of the inferior and superior reflections of the coronary ligaments. The right triangular ligament is formed by the fusion of the superior and inferior reflections of the right coronary ligament, separating the right subphrenic space from the right subhepatic space (the Morison pouch)[26].

The subhepatic space, comprising the lesser sac, is situated under the liver. The right subhepatic space extends medially through the foramen of Winslow to the lesser sac. The organs surrounding the lesser sac are the spleen on the left, the stomach and duodenum anterior and right, the transverse colon anterior, and the pancreas posterior.

The infra-mesocolic space is divided by the root of the small intestine mesentery into the right and the left infra-mesocolic space and into the pelvis[26,27]. The right infra-colic space is delimited by the caecum, the ascending colon, the mesoappendix and by the small bowel mesentery on the left. The ileum and the appendix always have a mesenterium. The caecum and the ascending colon are only partially covered by the peritoneum and their posterior face is frequently in contact with the posterior abdominal wall. However, it is possible to detect a true cecal mesentery. The left infra-colic space is situated between the small bowel mesentery and the mesentery of the descending colon and of the sigmoid colon. The sigmoid mesentery is situated obliquely in front of the ilio-sacral joint and this mesentery has a remarkable degree of mobility so that this bowel portion can be located in various sides within the peritoneal cavity.

The pelvic space is the most caudal space. The pelvis comprises anteriorly the bladder, part of which is covered by peritoneum. In women, the uterus and the tubes are situated within a large transverse peritoneal fold separating the pelvis into an anterior and posterior space. The pelvic space is divided ventrally by the remnant of the urachus (median umbilical ligament), the obliterated umbilical arteries (medial umbilical ligament), and the lateral umbilical ligaments (inferior epigastric vessels) into five fossae: the right and left lateral and medial inguinal fossae and the supravesical fossa. The peritoneal fossae of the pelvis extend laterally in the paravesical fossae, and dorsally, in the man, in the rectovesical fossa and, in the woman, in the cul-de-sac (Douglas pouch) and

the uterovesical fossa. The pelvic peritoneal space is normally occupied by small bowel loops[26,27].

The greater omentum, originating by the greater gastric curvature, divides the peritoneum in the frontal plane. It covers anteriorly most part of the infra-mesocolic compartment, crosses the transverse colon and falls in front of the abdominal viscera, sporadically down to the symphysis. The omental portion between the stomach and the colon is named the gastrocolic ligament, and the portion below the colon is the apron. The greater omentum forms the ligament between the spleen and stomach (gastrosplenic ligament) and connects the spleen to the dorsal abdominal wall.

The lesser omentum connects the small curvature of the stomach and the duodenal bulb to the inferior side of the liver. It is made by the gastrohepatic and hepatoduodenal ligaments, which are in anatomic continuity. The hepatoduodenal ligament comprises the portal vein, the hepatic artery and the common bile duct. The gastrohepatic ligament comprises the coronary vein and left gastric artery[26,27].

Imaging Tools

Imaging plays a critical role in the assessment of peritoneal illness. Evaluating disease burden is essential for HIPEC patient selection. A multimodality approach merges the strength of each imaging tool and improves diagnostic accuracy.

It is crucial to recognize that peritoneal imaging is a challenge due to the large extension of the peritoneum. In addition, peritoneal tumors can be imperceptible, even if widely distributed. Plain radiographs and barium studies have modest usefulness in PC. The diagnostic accuracy of abdominal radiographs is low[28], since it permits to assess indirect features as ascites, central displacement of small bowel, indistinct psoas margins, bulging of flanks and pleural effusion[28]. Ultrasound (US) has greater sensitivity to detect ascites: about 100 mL of intraperitoneal fluid, while radiography needs at least 500 mL[29]. The presence of indirect signs, on abdominal plain film, in patients at risk of PC, should be assessed with more sensitive tools, considering that the abdominal plain film is the first toll utilized in emergency setting[30-38]. Computed tomography (CT) is the best imaging tool for the assessment of known or suspected peritoneal implants. In fact, CT has exceptional spatial resolution. However, without contrast medium, the inadequate contrast resolution reduces its capacity to detect peritoneal tumour[36,39-41]. Coakley et al[42] showed that the sensitivity of CT for peritoneal tumors < 1 cm was only 25%-50% compared to 85%-93% for all tumors. So as, non-contrast enhanced T1-weighted (W) and T2-W Magnetic Resonance Imaging (MRI) performs poorly in detection of small peritoneal tumours[42]. MRI and CT have comparable accuracy in detection of PC and PC nodules size. In a study by Kim et al[43], it has been demonstrated that MRI shows a sensitivity of 95%. However, long breath holds, during MRI studies, are problematic for several cancer patients due to their usually frail states. These could cause artifacts reducing the quality of MRI evaluation[43,44]. Another MRI weakness is the presence of ascites, which could also lead to artifacts and then high wrong positive-rates[43]. A recent metanalysis[45], that involved 22 studies (934 assessed patients), revealed that MRI and CT have high per patient accuracy in detecting PC. However, due to the lack of evidence on MRI, the ideal imaging tool was CT. In the assessment of correspondence between Peritoneal Cancer Index (PCI) on CT and surgical PCI, the authors[45] found that CT seems to undervalue surgical PCI by about 12-33%.

Recent technical improvements in radiology have favored the use of dual-energy CT (DECT)[46-50]. Dual layer spectral detector CT (SDCT), the newly acquired dual-energy system, uses a single polychromatic x-ray source and identifies the photons of lower energies[51]. This allows dual-energy analysis to be performed on each data set acquired, which enables to generate spectral images such as virtual monoenergetic image (VMI). In several reports[52-55], VMIs have yielded high levels of contrast between iodine-enhanced tumors and neighboring tissues. Since peritoneal implants enhance with contrast media, low energy VMIs may be helpful for small peritoneal nodules evaluation. Kim et al[40] assessed quantitative and qualitative parameters of VMIs. To detect peritoneal implants, it is principally significant to maximize the contrast to noise ratio (CNR) and signal to noise ratio (SNR) during delayed phase of contrast studies. Kim et al[40] found that VMI at low energy levels produced substantially higher CNR and SNR values and superior lesion detection rate.

Clinical Setting

Ovarian Cancer

Ovarian cancer is the fourth leading cause of cancer deaths in women and is the most lethal of the gynecological malignancies. EOC is the typical tumor that spreads into peritoneum. It is appraised that 75% of women have advanced stage disease at the time of diagnosis[56], with peritoneal lesions (Figure 1). Patients with bulky abdominal tumor

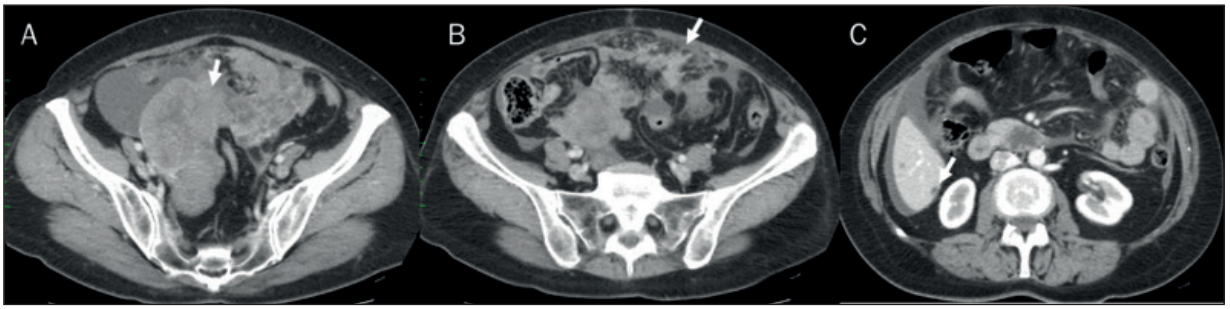

Figure 1. Patient with advanced ovarian cancer assessed on contrast Computed Tomography (CT) study. In **A**, the arrow shows the primary lesion, in **B** the arrow shows peritoneal involvement and in **C** subcapsular hepatic metastasis.

are treated with neoadjuvant chemotherapy to decrease tumor burden before surgery. Imaging is a useful tool to direct biopsies in patients with more limited metastatic tumour[57-59].

Although, there is no strong agreement on the resectability criteria of PC, massive involvement of the small bowel or mesenteric root, so as involved of lymph nodes superior to the celiac axis, pleural infiltration, pelvic sidewall invasion, bladder trigone involvement, and hepatic parenchymal metastases or implants near the right hepatic vein are thought indicative signs of non-resectability[57]. The pre-surgical staging of liver is critical for treatment planning[60-64]. The radiologist's report should specify the size, side, and number of implants on the liver. The presence of subcapsular implants in the region extending from the Morison pouch to the inferior vena cava at the level of the right hepatic vein should be reported since it causes an increased risk of intraoperative bleeding precluding optimal debulking[57,65-70].

CT is the diagnostic tool of choice for the assessment of OC with an accuracy of 70%-90% for the detection of lesion at all disease stages. Moreover, it has been showed to be an accurate technique for predicting surgical cytoreduction outcome[42]. The most important weakness of CT is its incapability to detect lesions with a maximal diameter of less than 5 mm on the bowel serosa and mesentery specially in absence of ascites[42].

Gastrointestinal Cancers

Gastric cancer (Figure 2) and CRC usually spread into the peritoneal cavity. In CRC, the risk features associated with PC are right-sided tumor (Figure 3), mucinous type, patients younger than 70-75 years, emergency surgery at diagnosis, and partial primary tumor resection[1,2,71,72].

The Krukenberg tumor is the involvement of ovaries in GC[2,73]. It is much more usual to appreciate implants involving free peritoneal surfaces, omen-

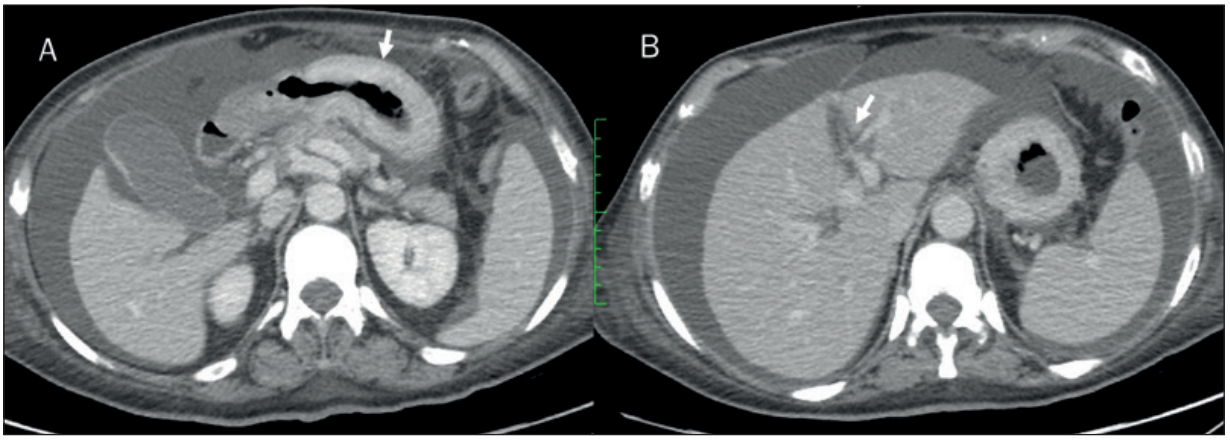

Figure 2. Patient assessed on contrast CT study with Gastric Cancer (**A**; arrow) and PC with peribiliary and falciform ligament involvement (**B**; arrow).

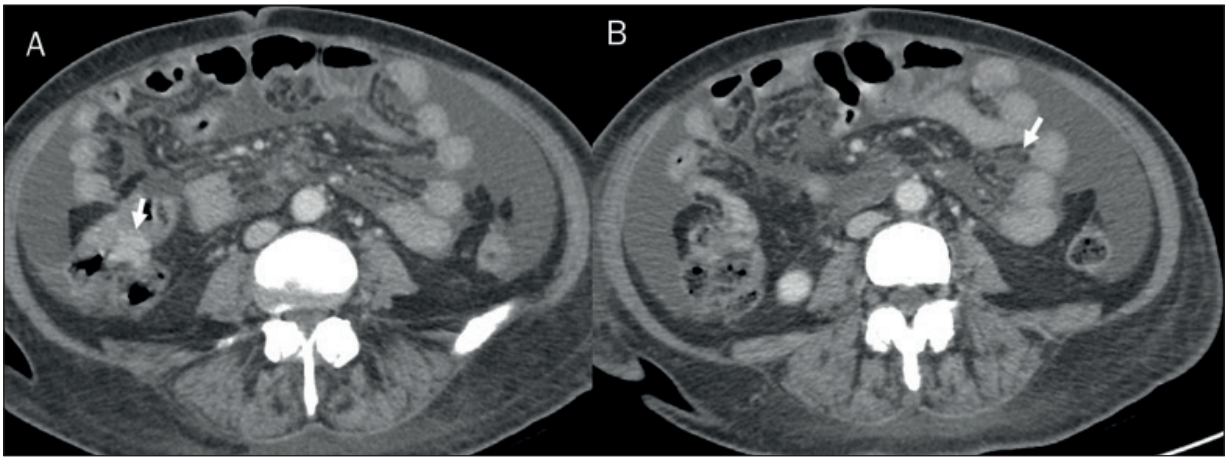

Figure 3. Patient with Right Colon Cancer assessed on contrast CT study. In **A**, the arrow shows the primary lesion and in **B** disseminate peritoneal involvement.

tum and upper abdominal peritoneal reflections. Advanced GC should cause small bowel obstruction due to disseminated peritoneal tumor. Alike, Stage IV CRC should present with peritoneal lesions involving the pelvis, free peritoneal surfaces, omentum, mesentery and bowel serosa. Recurrence of gastrointestinal tumor often affects the peritoneum. It is assessed that 20%-50% of recurrences by CRC affects peritoneal cavity (Figure 4)[1,2].

Pseudomyxoma peritonei (PMP) is an uncommon tumor in which gelatinous ascites spreads in the peritoneal cavity. The main cause of PMP is perforation of an appendicular mucinous tumour. In the past, PMP was treated with frequent drainage of mucinous ascites; today, CRS plus HIPEC has been recognised as the standard of care[1,2]. The typical imaging findings[74,75] include a cystic and solid mass in abdominal cavity, peritoneum and omentum thickening, calcification foci in the abdominal cavity, enlarged abdominal lymph nodes, small bowel displacement.

In pancreatic cancer patients, peritoneal metastases are present in 22%-48% of cases without detectable lesions on CT[76-80]. Microscopic tumor could be established by cytologic assessment of peritoneal fluid[76,82]. The detection of peritoneal lesions on contrast studies can change patient treatment by precluding surgery in a patient with resectable lesions (Figure 5 and Figure 6). Peritoneal implants are also frequently found in cholangiocarcinoma (Figure 7 and Figure 8)[83,84], endometrial cancer (Figure 9) and gastrointestinal car-

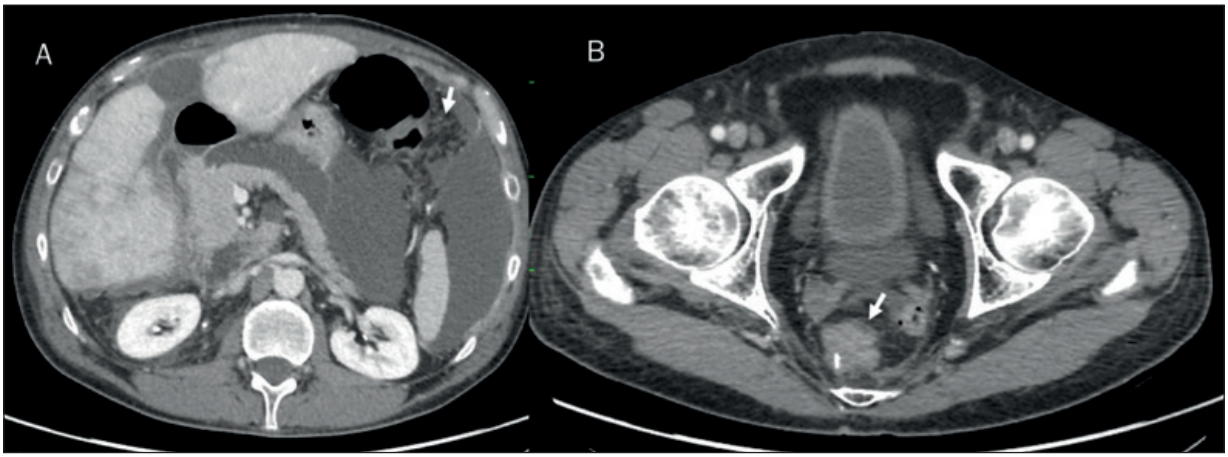

Figure 4. Patient subjected to mesorectal cancer excision with recurrence in peritoneal (in **A**, the arrow shows PC) and in pelvis side (in **B**, the arrow shows recurrence), assessed on contrast CT study.

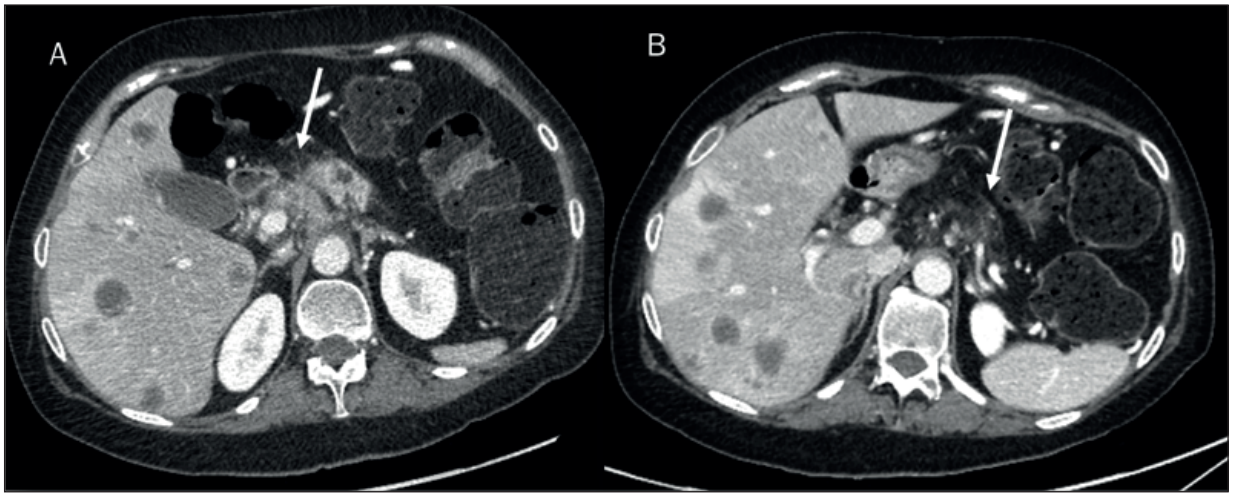

Figure 5. Patient with pancreatic cancer assessed on contrast CT study. In **A** and **B**, the arrow shows PC.

cinoid tumours[84-89]. Extra abdominal tumors with widespread spreading can also comprise peritoneal cavity[90-93].

Qualitative Assessment

Peritoneal implants are solid with heterogeneous enhancement and may have the shape of nodules, plaques or masses. Sporadically, multiple tiny lesions may be shown as fat stranding. Widespread tiny lesions covering the parietal peritoneum may be seen as thickening and enhancement of parietal peritoneum. Peritoneal implants may infrequently be cystic, when the primary tumor is a mucinous carcinoma. In this case, the lesions could mimic a loculated fluid. Calcifications of peritoneal lesions could be found when the primary lesion is either serous ovarian cystadenocarcinoma or GC[92,94,95].

When lesions cover the peritoneal surface of the liver and spleen, they may indent the parenchyma generating a "scalloping" appearance[93].

The presence of ascites could help in detecting of peritoneal tumors, even if small peritoneal implants, lesser than 1 cm, could be not assessed on unenhanced imaging studies[42].

On contrast studies, lesions on collapsed or partially distended intestinal loops may be challenging to be detected. Adequate small bowel (SB) loop distention is required for the detection of small lesions on the intestinal wall. Implants located on SB wall may be nodules or masses between and should cause bowel obstruction. Multiple tiny implants covering the surface of the SB loops may be

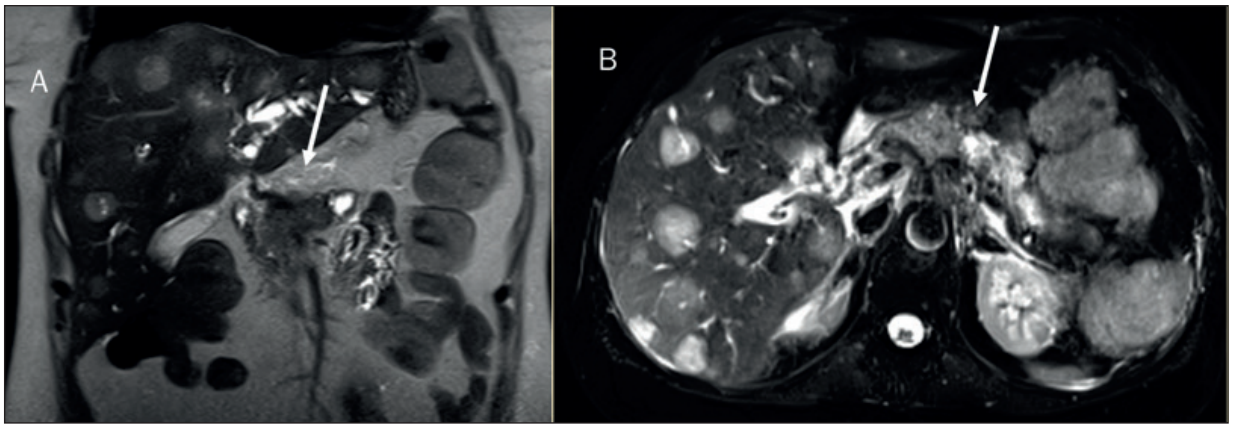

Figure 6. The same patient of Figure 5, assessed on MRI (in **A** T2-W sequence in coronal plane and in **B** T2-W FAT Suppressed sequence in axial plane). The PC is not as well evident as in CT study.

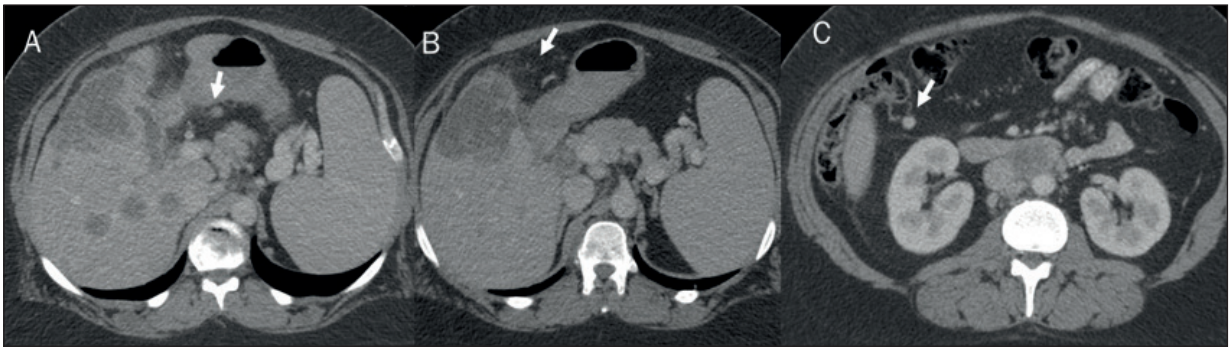

Figure 7. Patient with Mass Forming Intrahepatic Cholangiocarcinoma assessed on contrast CT study. The arrow (in **A-C**) shows peritoneal involvement.

seen as wall enhanced thickening, so as restricted distensibility and distortion of SB segments with intestinal stenosis. The terminal ileum and the first jejunum loop are critical parts to evaluate: mesenteric enhancement is a valuable sign of peritoneal involvement. Peritoneal implants usually enhance slowly with contrast medium. Small peritoneal tumors and peritoneal carcinomatosis are clearly detected on images obtained 5-10 min following injection of contrast medium[7,9].

MRI should be chosen for lesions in the right subphrenic space. Any enhancing tumors between the face of the liver and the adjacent right hemidiaphragm are clearly detected. These tumors may present as nodules or masses, or as abnormal enhancement of the non-thickened or thickened right hemidiaphragm[96-99]. These features should be found in left subphrenic tumors. Also, implants should be adjacent to the spleen or stomach[93]. On diffusion weighted images (DWI) using a b value of 300–500 s/mm^2, peritoneal implants show restricted diffusion[96-101].

Peritoneal implants on the gallbladder and on the peritoneum lining the gallbladder fossa should be detected as mural enhanced thickening[102-105].

Semiquantitative Assessment

Peritoneal cancer index (PCI) is a quantitative index suggested by Harman and Sugarbaker to define the extent of PC. It reveals the lesions site and size[106,107]. This value reproduces the Gilly's cancer stage, SPCI stage in the Netherlands, and P stage for peritoneal lesions of GC in Japan[108]. The outcomes of PC are largely related to the tumor spread, localization, and size. Accurate evaluation of these factors is very critical for determining prognosis and therapeutic approach. Patients with a PCI over 20 are considered not to be qualified for cytoreductive surgery[109].

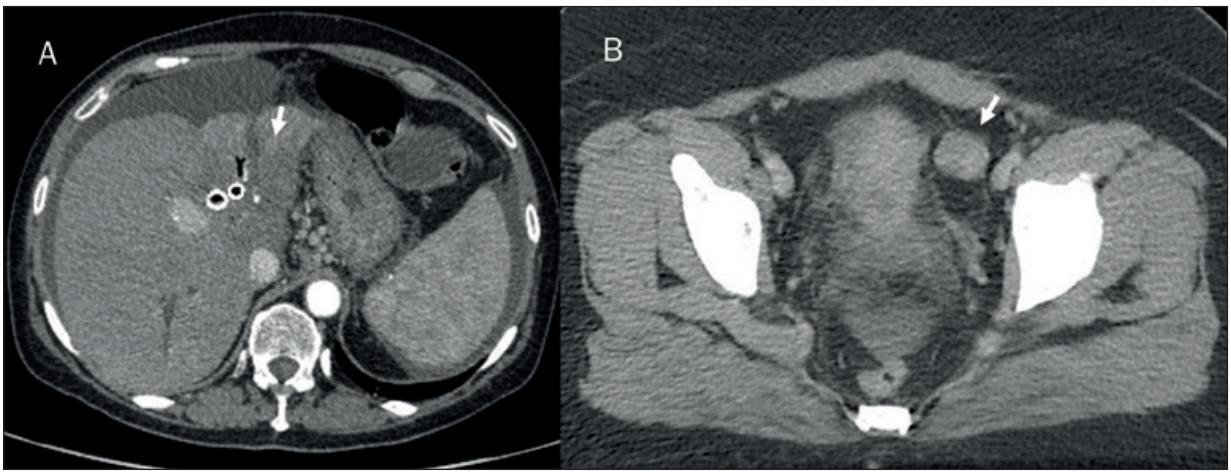

Figure 8. Patient with Periductal Cholangiocarcinoma assessed on contrast CT study. In **A**, the arrow shows the primary lesion and in **B** the ovarian involvement.

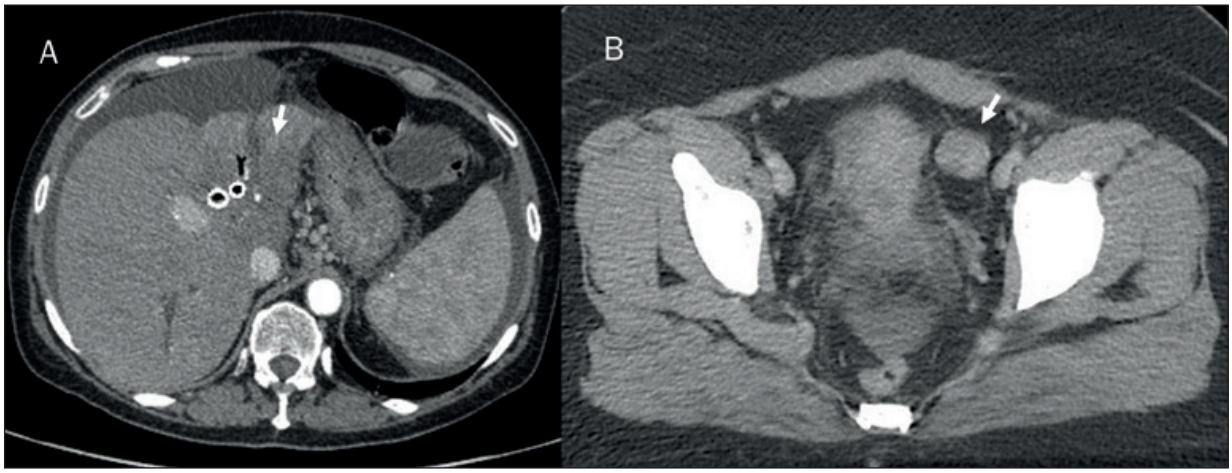

Figure 9. Patient with Endometrial Cancer assessed on contrast CT study. In **A**, the arrow shows the primary lesion and in **B** the peritoneal involvement.

To assess the PCI, the entire abdominal and intestinal area is divided into 13 areas:

- R0: Middle abdomen, including the greater omentum and transverse colon;
- R1: Right upper, including the right upper liver, right inferior diaphragmatic surface, and upper posterior surface of the right liver;
- R2: Epigastrium, including the left hepatic lobe, lesser omentum, falciform ligament, and upper abdominal fat pad;
- R3: Left upper, including the spleen, tail of pancreas, stomach, and left inferior diaphragmatic surface;
- R4: Left flank, including the descending colon and left ventral groove;
- R5: Left lower, including the sigmoid colon and lateral wall of the left pelvis;
- R6: Pelvis, including the female internal genital organs, bladder, sigmoid colon, and Douglas bag;
- R7: Right lower, including the cecum, vermiform appendix, and lateral wall of the right pelvis;
- R8: Right flank, including the ascending colon and right abdominal cavity;
- R9: Upper jejunum;
- R10: Lower jejunum;
- R11: Upper ileum;
- R12: Lower ileum.

In each of the 13 areas the maximum visible lesion size is assessed and, according to it, it is assigned a score between LS = 0 and LS = 3 (LS = 0 means no tumor visible, LS = 1 means a tumor lesion size below 0.5 cm, LS = 2 means a tumor lesion size between 0.5 cm and 5 cm, and LS = 3 means a tumor lesion size larger than 5 cm or describes a confluent tumors).

Assessment of PCI score is correlated to the expertise of the radiologist. A study by Coakley et al[42], in which preoperative CT of ovarian carcinoma patients were assessed by three independent readers, showed that the detection of peritoneal lesions was good to excellent. This study showed an overall sensitivity of 94% and specificity of 80% which were in line with more recent studies[109]: patients with a PCI score of less than or equal to 10 have a 5-year survival rate of 50%, while survival rates of 20% and 0% for scores between 11 and 20, and over 20, respectively.

CT is usually performed to assess the PCI. A limit of CT is a low diagnostic accuracy in discriminating the tumor scar tissue from the post-surgical scar tissue[45]. Also, there are several weaknesses due to the known limits of PCI staging system. For example, the confines between the 13 areas are unclear, specifically for small bowel and more implants in a single area led to the same score for a single lesion of the same size. Moreover, diverse implants aspects improve the problems to detect PC and, therefore, the probability of imprecise tumor assessment[45]. Also, the assessment of several critical structures, as the first jejunal loop, the falciform ligament or the hepatic hilum, should be evaluated with a different weight, as they can impact on the surgical choice[45].

Radiomics and PCI

Radiomics is a developing field, mainly in the oncological setting[110-116]. Manual segmentation is one of the main critical moments of radiomics analysis. It could be time-consuming and could suffer from variability in tumor delineation. Radiomic features provides data on tumor phenotype as well as microenvironment[117-128]. Radiomics-derived parameters, when correlated with clinical data and outcomes, could generate accurate robust evidence-based clinical-decision support systems (CDSS)[129-147].

The central idea of radiomics is that quantitative voxel-based variables are more significantly correlated with various clinical end points respect to the qualitative radiologic assessment[62]. In fact, Radiomics data provide important benefits, since this analysis is not related to the subjected evaluation. An increase of radiomics could be due adding these data to others prognostic markers, as genomics. Radiogenomics is an evolving prognostic tool; in fact, these biomarkers have been found to relate with treatment response, metastatic spread, and prognosis[62,64,138-157].

Song et al[117] validated MRI-based radiomics signature for the individualized preoperative prediction of PC in OC. They selected 6 features and showed a positive capacity to predict PC with an area under the curve (AUC) of 0.963 in the training cohort and an AUC of 0.928 in the validation cohort. The results by Song et al[117] confirmed the thesis that radiomics signatures could predict PC through capture tumoral heterogeneity differences between ovarian cancers[117].

Conclusions

Imaging plays a critical role in the PC assessment. These data facilitate staging, guide management, and determine prognosis. Evaluating disease burden is crucial for treatment selection. A multimodality imaging approach, combining the strength of each imaging tools, should be considered, even if the preferred imaging tool is CT. The outcomes of PC are mainly associated with tumor spread, localization, and size. Accurate assessment of these data is therefore critical for determining therapeutic approach. These data can be described by PCI, a quantitative index suggested by Harman and Sugarbaker.

Accurate predictive biomarkers should be established to predict PC in patients at risk. The radiomics signatures could predict PC through capture tumoral heterogeneity differences between lesions with or without PC.

Acknowledgements

The authors are grateful to Alessandra Trocino, librarian at the National Cancer Institute of Naples, Italy. Moreover, for the collaboration, authors are grateful to Paolo Pariate, Martina Totaro and Andrea Esposito for the research support of Radiology Division, "Istituto Nazionale Tumori IRCCS Fondazione Pascale – IRCCS di Napoli", Naples, Italy.

Data Availability

Data are available at link https://zenodo.org/record/5931374#.Yjx6j-fMK3B.

Conflict of Interest

The authors have no conflict of interest to be disclosed. The authors confirm that the article is not under consideration for publication elsewhere. Each author has participated sufficiently to take public responsibility for the manuscript content.

References

1) Coccolini F, Gheza F, Lotti M, Virzì S, Iusco D, Ghermandi C, Melotti R, Baiocchi G, Giulini SM, Ansaloni L, Catena F. Peritoneal carcinomatosis. World J Gastroenterol 2013; 19: 6979-6994.
2) Lemoine L, Sugarbaker P, Van der Speeten K. Pathophysiology of colorectal peritoneal carcinomatosis: role of the peritoneum. World J Gastroenterol 2016; 22: 7692-7707.
3) Avesani G, Arshad M, Lu H, Fotopoulou C, Cannone F, Melotti R, Aboagye E, Rockall A. Radiological assessment of Peritoneal Cancer Index on preoperative CT in ovarian cancer is related to surgical outcome and survival. Radiol Med 2020; 125: 770-776.
4) Llueca A, Serra A, Rivadulla I, Gomez L, Escrig J. MUAPOS working group (Multidisciplinary Unit of Abdominal Pelvic Oncology Surgery). Prediction of suboptimal cytoreductive surgery in patients with advanced ovarian cancer based on preoperative and intraoperative determination of the peritoneal carcinomatosis index. World J Surg Oncol 2018; 16: 37.
5) Bertocchi E, Barugola G, Nicosia L, Mazzola R, Ricchetti F, Dell'Abate P, Alongi F, Ruffo G. A comparative analysis between radiation dose intensification and conventional fractionation in neoadjuvant locally advanced rectal cancer: a monocentric prospective observational study. Radiol Med 2020; 125: 990-998.
6) Elmohr MM, Elsayes KM, Pickhardt PJ. Non-neoplastic conditions mimicking peritoneal carci-

nomatosis at CT imaging. Br J Radiol 2020; 93: 20200401.

7) Vicens RA, Patnana M, Le O, Bhosale PR, Sagebiel TL, Menias CO, Balachandran A. Multimodality imaging of common and uncommon peritoneal diseases: a review for radiologists. Abdom Imaging 2015; 40: 436-456.
8) Cutaia G, Tosto G, Cannella R, Bruno A, Leto C, Salvaggio L, Cutaia S, Lombardo FP, Dispensa N, Giambelluca D, Midiri M, Salvaggio G. Prevalence and clinical significance of incidental findings on multiparametric prostate MRI. Radiol Med 2020; 125: 204-213.
9) Diop AD, Fontarensky M, Montoriol PF, Da Ines D. CT imaging of peritoneal carcinomatosis and its mimics. Diagn Interv Imaging 2014; 95: 861-872.
10) Pickhardt PJ, Perez AA, Elmohr MM, Elsayes KM. CT imaging review of uncommon peritoneal-based neoplasms: beyondcarcinomatosis. Br J Radiol 2021; 94: 20201288.
11) Quénet F, Elias D, Roca L, Goéré D, Ghouti L, Pocard M, Facy O, Arvieux C, Lorimier G, Pezet D, Marchal F, Loi V, Meeus P, Juzyna B, de Forges H, Paineau J, Glehen O; UNICANCER-GI Group and BIG Renape Group. Cytoreductive surgery plus hyperthermic intraperitoneal chemotherapy versus cytoreductive surgery alone for colorectal peritoneal metastases (PRODIGE 7): a multicentre, randomised, open-label, phase 3 trial. Lancet Oncol 2021; 22: 256-266.
12) Sánchez-Hidalgo JM, Rodríguez-Ortiz L, Arjona-Sánchez Á, Rufián-Peña S, Casado-Adam Á, Cosano-Álvarez A, Briceño-Delgado J. Colorectal peritoneal metastases: Optimal management review. World J Gastroenterol 2019; 25: 3484-3502.
13) Cortes-Guiral D, Glehen O. Expanding Uses of HIPEC for Locally Advanced Colorectal Cancer: A European Perspective. Clin Colon Rectal Surg 2020; 33: 253-257.
14) Petralia G, Summers PE, Agostini A, Ambrosini R, Cianci R, Cristel G, Calistri L, Colagrande S. Dynamic contrast-enhanced MRI in oncology: how we do it. Radiol Med 2020; 125: 1288-1300.
15) Dohan A, Hobeika C, Najah H, Pocard M, Rousset P, Eveno C. Preoperative assessment of peritoneal carcinomatosis of colorectal origin. J Visc Surg 2018; 155: 293-303.
16) Oei TN, Jagannathan JP, Ramaiya N, Ros PR. Peritoneal sarcomatosis versus peritoneal carcinomatosis: imaging findings at MDCT. AJR Am J Roentgenol 2010; 195: W229-W235.
17) Ria F, Samei E. Is regulatory compliance enough to ensure excellence in medicine? Radiol Med 2020; 125: 904-905.
18) Cabral FC, Krajewski KM, Kim KW, Ramaiya NH, Jagannathan JP. Peritoneal lymphomatosis: CT and PET/CT findings and how to differentiate between carcinomatosis and sarcomatosis. Cancer Imaging 2013; 13: 162-170.
19) Sia DS, Kapur J, Thian YL. Peritoneal lymphomatosis mimicking peritoneal carcinomatosis: important imaging clues for correct diagnosis. Singapore Med J 2013; 54: e93-e96.
20) Zhang A, Song J, Ma Z, Chen T. Combined dynamic contrast-enhanced magnetic resonance imaging and diffusion-weighted imaging to predict neoadjuvant chemotherapy effect in FIGO stage IB2-IIA2 cervical cancers. Radiol Med 2020; 125: 1233-1242.
21) Jayne D. Molecular biology of peritoneal carcinomatosis. Cancer Treat Res 2007; 134: 21-33.
22) Rega D, Pace U, Scala D, Chiodini P, Granata V, Fares Bucci A, Pecori B, Delrio P. Treatment of splenic flexure colon cancer: a comparison of three different surgical procedures: Experience of a high volume cancer center. Sci Rep 2019; 9: 10953.
23) Rega D, Granata V, Petrillo A, Pace U, Sassaroli C, Di Marzo M, Cervone C, Fusco R, D'Alessio V, Nasti G, Romano C, Avallone A, Pecori B, Botti G, Tatangelo F, Maiolino P, Delrio P. Organ Sparing for Locally Advanced Rectal Cancer after Neoadjuvant Treatment Followed by Electrochemotherapy. Cancers (Basel) 2021; 13: 3199.
24) Granata V, Faggioni L, Grassi R, Fusco R, Reginelli A, Rega D, Maggialetti N, Buccicardi D, Frittoli B, Rengo M, Bortolotto C, Prost R, Lacasella GV, Montella M, Ciaghi E, Bellifemine F, De Muzio F, Grazzini G, De Filippo M, Cappabianca S, Laghi A, Grassi R, Brunese L, Neri E, Miele V, Coppola F. Structured reporting of computed tomography in the staging of colon cancer: a Delphi consensus proposal. Radiol Med 2022; 127: 21-29.
25) Giurazza F, Corvino F, Silvestre M, Cangiano G, De Magistris G, Cavaglià E, Amodio F, Niola R. Embolization of peripheral arteriovenous malformations and fistulas with precipitating hydrophobic injectable liquid (PHIL®). Radiol Med 2021; 126: 474-483.
26) Solass W, Struller F, Horvath P, Königsrainer A, Sipos B, Weinreich FJ. Morphology of the peritoneal cavity and pathophysiological consequences. Pleura Peritoneum 2016; 1: 193-201.
27) Raptopoulos V, Gourtsoyiannis N. Peritoneal carcinomatosis. Eur Radiol 2001; 11: 2195-2206.
28) Bundrick TJ, Cho SR, Brewer WH, Beachley MC. Ascites: comparison of plain film radiographs with ultrasonograms. Radiology 1984; 152: 503-506.
29) Forshee WA, DiSantis DJ, McComb BL. The floating bowel sign. Abdom Radiol (NY) 2018; 43: 1837-1838.
30) Trinci M, Cirimele V, Cozzi D, Galluzzo M, Miele V. Diagnostic accuracy of pneumo-CT-cystography in the detection of bladder rupture in patients with blunt pelvic trauma. Radiol Med 2020; 125: 907-917.
31) Giovagnoni, A. Facing the COVID-19 emergency: we can and we do. Radiol Med 2020; 125: 337-338.
32) Russo L, Gui B, Miccò M, Panico C, De Vincenzo R, Fanfani F, Scambia G, Manfredi R. The role of MRI in cervical cancer>2 cm (FIGO stage IB2-IIA1) conservatively treated with neoadjuvant chemotherapy followed by conization: a pilot study. Radiol Med 2021; 126: 1055-1063.
33) Hussein MAM, Cafarelli FP, Paparella MT, Rennie WJ, Guglielmi G. Phosphaturic mesenchymal tumors:

radiological aspects and suggested imaging pathway. Radiol Med 2021; 126: 1609-1618.

34) Sureka B, Meena V, Garg P, Yadav T, Khera PS. Computed tomography imaging of ovarian peritoneal carcinomatosis: a pictorial review. Pol J Radiol 2018; 83: e500-e509.

35) Roze JF, Hoogendam JP, van de Wetering FT, Spijker R, Verleye L, Vlayen J, Veldhuis WB, Scholten RJ, Zweemer RP. Positron emission tomography (PET) and magnetic resonance imaging (MRI) for assessing tumour resectability in advanced epithelial ovarian/fallopian tube/primary peritoneal cancer. Cochrane Database Syst Rev 2018; 10: CD012567.

36) Low RN. MR imaging of the peritoneal spread of malignancy. Abdom Imaging 2007; 32: 267-283.

37) Batouty NM, Sobh DM, Gadelhak B, Sobh HM, Mahmoud W, Tawfik AM. Left superior vena cava: cross-sectional imaging overview. Radiol Med 2020; 125: 237-246.

38) Bottari A, Silipigni S, Carerj ML, Cattafi A, Maimone S, Marino MA, Mazziotti S, Pitrone A, Squadrito G, Ascenti G. Dual-source dual-energy CT in the evaluation of hepatic fractional extracellular space in cirrhosis. Radiol Med 2020; 125: 7-14.

39) Choi HJ, Lim MC, Bae J, Cho KS, Jung DC, Kang S, Yoo CW, Seo SS, Park SY. Region-based diagnostic performance of multidetector CT for detecting peritoneal seeding in ovarian cancer patients. Arch Gynecol Obstetr 2011; 283: 353-360.

40) Kim TM, Kim SY, Cho JY, Kim SH, Moon MH. Utilization of virtual low-keV monoenergetic images generated using dual-layer spectral detector computed tomography for the assessment of peritoneal seeding from ovarian cancer. Medicine (Baltimore) 2020; 99: e20444.

41) Nougaret S, Addley HC, Colombo PE, Fujii S, Al Sharif SS, Tirumani SH, Jardon K, Sala E, Reinhold C. Ovarian carcinomatosis: how the radiologist can help plan the surgical approach. Radiographics 2012; 32: 1775-800.

42) Coakley FV, Choi PH, Gougoutas CA, Pothuri B, Venkatraman E, Chi D, Bergman A, Hricak H. Peritoneal metastases: detection with spiral CT in patients with ovarian cancer. Radiology 2002; 223: 495-499.

43) Kim CK, Park BK. Comparison of the MRI and integrated PET/CT findings in the preoperative detection of peritoneal carcinomatosis arising from primary ovarian cancer. J Korean Soc Radiol 2009; 60: 117-126.

44) Crimì F, Capelli G, Spolverato G, Bao QR, Florio A, Milite Rossi S, Cecchin D, Albertoni L, Campi C, Pucciarelli S, Stramare R. MRI T2-weighted sequences-based texture analysis (TA) as a predictor of response to neoadjuvant chemo-radiotherapy (nCRT) in patients with locally advanced rectal cancer (LARC). Radiol Med 2020; 125: 1216-1224.

45) Laghi A, Bellini D, Rengo M, Accarpio F, Caruso D, Biacchi D, Di Giorgio A, Sammartino P. Diagnostic performance of computed tomography and magnetic resonance imaging for detecting peritoneal metastases: systematic review and meta-analysis. Radiol Med 2017; 122: 1-15.

46) Agostini A, Floridi C, Borgheresi A, Badaloni M, Esposto Pirani P, Terilli F, Ottaviani L, Giovagnoni A. Proposal of a low-dose, long-pitch, dual-source chest CT protocol on third-generation dual-source CT using a tin filter for spectral shaping at 100 kVp for Corona-Virus Disease 2019 (COVID-19) patients: a feasibility study. Radiol Med 2020; 125: 365-373.

47) Bottari A, Silipigni S, Carerj ML, Cattafi A, Maimone S, Marino MA, Mazziotti S, Pitrone A, Squadrito G, Ascenti G. Dual-source dual-energy CT in the evaluation of hepatic fractional extracellular space in cirrhosis. Radiol Med 2020; 125: 7-14.

48) Granata V, Grassi R, Fusco R, Galdiero R, Setola SV, Palaia R, Belli A, Silvestro L, Cozzi D, Brunese L, Petrillo A, Izzo F. Pancreatic cancer detection and characterization: state of the art and radiomics. Eur Rev Med Pharmacol Sci 2021; 25: 3684-3699.

49) Uhrig M, Simons D, Kachelrieß M, Pisana F, Kuchenbecker S, Schlemmer HP. Advanced abdominal imaging with dual energy CT is feasible without increasing radiation dose. Cancer Imaging 2016; 16: 15.

50) Siegel MJ, Curtis WA, Ramirez-Giraldo JC. Effects of Dual-Energy Technique on Radiation Exposure and Image Quality in Pediatric Body CT. AJR Am J Roentgenol 2016; 207: 826-835.

51) Granata V, Grassi R, Fusco R, Setola SV, Palaia R, Belli A, Miele V, Brunese L, Grassi R, Petrillo A, Izzo F. Assessment of Ablation Therapy in Pancreatic Cancer: The Radiologist's Challenge. Front Oncol 2020; 10: 560952.

52) Granata V, Fusco R, Avallone A, Catalano O, Piccirillo M, Palaia R, Nasti G, Petrillo A, Izzo F. A radiologist's point of view in the presurgical and intraoperative setting of colorectal liver metastases. Future Oncol 2018; 14: 2189-2206.

53) Granata V, Grassi R, Fusco R, Belli A, Palaia R, Carrafiello G, Miele V, Grassi R, Petrillo A, Izzo F. Local ablation of pancreatic tumors: State of the art and future perspectives. World J Gastroenterol 2021; 27: 3413-3428.

54) Granata V, Fusco R, Salati S, Petrillo A, Di Bernardo E, Grassi R, Palaia R, Danti G, La Porta M, Cadossi M, Gašljević G, Sersa G, Izzo F. A Systematic Review about Imaging and Histopathological Findings for Detecting and Evaluating Electroporation Based Treatments Response. Int J Environ Res Public Health 2021; 18: 5592.

55) Esposito A, Gallone G, Palmisano A, Marchitelli L, Catapano F, Francone M. The current landscape of imaging recommendations in cardiovascular clinical guidelines: toward an imaging-guided precision medicine. Radiol Med 2020; 125: 1013-1023.

56) Levy AD, Arnáiz J, Shaw JC, Sobin LH. From the archives of the AFIP: primary peritoneal tumors: imaging features with pathologic correlation. Radiographics 2008; 28: 583-607.

57) Qi Z, Zhang Y, Dai Q, Xia Y, Jiang Y. Peritoneal Carcinomatosis in Primary Ovarian Cancer: Ultrasound Detection and Comparison with Computed Tomography. Ultrasound Med Biol 2017; 43: 1811-1819.

58) Granata V, Bicchierai G, Fusco R, Cozzi D, Grazzini G, Danti G, De Muzio F, Maggialetti N, Smorchkova O, D'Elia M, Brunese MC, Grassi R, Giacobbe G, Bruno F, Palumbo P, Grassi F, Brunese L, Grassi R, Miele V, Barile A. Diagnostic protocols in oncology: workup and treatment planning. Part 2: Abbreviated MR protocol. Eur Rev Med Pharmacol Sci 2021; 25: 6499-6528.

59) Panagiotopoulou PB, Courcoutsakis N, Tentes A, Prassopoulos P. CT imaging of peritoneal carcinomatosis with surgical correlation: a pictorial review. Insights Imaging 2021; 12: 168.

60) Le O. Patterns of peritoneal spread of tumor in the abdomen and pelvis. World J Radiol 2013; 5: 106-112.

61) Sharma M, Patil A, Kumar A, Pathak A, Somani P, Sreesh SS, Rameshbabu CS. Imaging of infracolic and pelvic compartment by linear EUS. Endosc Ultrasound 2019; 8: 161-171.

62) Granata V, Fusco R, Avallone A, De Stefano A, Ottaiano A, Sbordone C, Brunese L, Izzo F, Petrillo A. Radiomics-Derived Data by Contrast Enhanced Magnetic Resonance in RAS Mutations Detection in Colorectal Liver Metastases. Cancers (Basel) 2021; 13: 453.

63) Granata V, Fusco R, Avallone A, Cassata A, Palaia R, Delrio P, Grassi R, Tatangelo F, Grazzini G, Izzo F, Petrillo A. Abbreviated MRI protocol for colorectal liver metastases: How the radiologist could work in pre surgical setting. PLoS One 2020; 15: e0241431.

64) Granata V, Fusco R, Risi C, Ottaiano A, Avallone A, De Stefano A, Grimm R, Grassi R, Brunese L, Izzo F, Petrillo A. Diffusion-Weighted MRI and Diffusion Kurtosis Imaging to Detect RAS Mutation in Colorectal Liver Metastasis. Cancers (Basel) 2020; 12: 2420.

65) Abdalla Ahmed S, Abou-Taleb H, Ali N, M Badary D. Accuracy of radiologic-laparoscopic peritoneal carcinomatosis categorization in the prediction of surgical outcome. Br J Radiol 2019; 92: 20190163.

66) Chandramohan A, Bhat TA, John R, Simon B. Multimodality imaging review of complex pelvic lesions in female pelvis. Br J Radiol 2020; 93: 20200489.

67) Rodolfino E, Di Marco M, Ilot A, Iezzi R, Gui B, Avesani G, Panico C, Strippoli A, Di Giorgio A, Pacelli F, Manfredi R. Radiologist Checklist for Selecting Patients to Undergo PIPAC (Pressurized IntraPeritoneal Aerosol Chemotherapy). Life (Basel) 2021; 11: 941.

68) Batouty NM, Sobh DM, Gadelhak B, Sobh HM, Mahmoud W, Tawfik AM. Left superior vena cava: cross-sectional imaging overview. Radiol Med 2020; 125: 237-246.

69) Granata V, Fusco R, Maio F, Avallone A, Nasti G, Palaia R, Albino V, Grassi R, Izzo F, Petrillo A. Qualitative assessment of EOB-GD-DTPA and Gd-BT-DO3A MR contrast studies in HCC patients and colorectal liver metastases. Infect Agent Cancer 2019; 14: 40.

70) Mazzola R, Cuccia F, Figlia V, Rigo M, Nicosia L, Giaj-Levra N, Ricchetti F, Vitale C, Mantoan B, Di Paola G, De Simone A, Gurrera D, Sicignano G, Naccarato S, Ruggieri R, Alongi F. Stereotactic body radiotherapy for oligometastatic castration sensitive prostate cancer using 1.5 T MRI-Linac: preliminary data on feasibility and acute patient-reported outcomes. Radiol Med 2021; 126: 989-997.

71) Rega D, Pace U, Scala D, Chiodini P, Granata V, Fares Bucci A, Pecori B, Delrio P. Treatment of splenic flexure colon cancer: a comparison of three different surgical procedures: Experience of a high volume cancer center. Sci Rep 2019; 9: 10953.

72) Miraglia R, Maruzzelli L, Cannataci C, Gerasia R, Mamone G, Cortis K, Cimò B, Petridis I, Volpes R, Luca A. Radiation exposure during transjugular intrahepatic portosystemic shunt creation in patients with complete portal vein thrombosis or portal cavernoma. Radiol Med 2020; 125: 609-617.

73) De Vuysere S, Vandecaveye V, De Bruecker Y, Carton S, Vermeiren K, Tollens T, De Keyzer F, Dresen RC. Accuracy of whole-body diffusion-weighted MRI (WB-DWI/MRI) in diagnosis, staging and follow-up of gastric cancer, in comparison to CT: a pilot study. BMC Med Imaging 2021; 21:18.

74) Menassel B, Duclos A, Passot G, Dohan A, Payet C, Isaac S, Valette PJ, Glehen O, Rousset P. Preoperative CT and MRI prediction of non-resectability in patients treated for pseudomyxoma peritonei from mucinous appendiceal neoplasms. Eur J Surg Oncol 2016; 42: 558-566.

75) Lee NK, Kim S, Kim HS, Jeon TY, Kim GH, Kim DU, Park DY, Kim TU, Kang DH. Spectrum of mucin-producing neoplastic conditions of the abdomen and pelvis: cross-sectional imaging evaluation. World J Gastroenterol 2011; 17: 4757-4771.

76) Izzo F, Granata V, Fusco R, D'Alessio V, Petrillo A, Lastoria S, Piccirillo M, Albino V, Belli A, Nasti G, Avallone A, Patrone R, Grassi F, Leongito M, Palaia R. A Multicenter Randomized Controlled Prospective Study to Assess Efficacy of Laparoscopic Electrochemotherapy in the Treatment of Locally Advanced Pancreatic Cancer. J Clin Med 2021; 10: 4011.

77) Garcia-Sampedro A, Gaggia G, Ney A, Mahamed I, Acedo P. The State-of-the-Art of Phase II/III Clinical Trials for Targeted Pancreatic Cancer Therapies. J Clin Med 2021; 10: 566.

78) Souza D, Alessandrino F, Ketwaroo GA, Sawhney M, Mortele KJ. Accuracy of a novel noninvasive secretin-enhanced MRCP severity index scoring system for diagnosis of chronic pancreatitis: correlation with EUS-based Rosemont criteria. Radiol Med 2020; 125: 816-826.

79) Srisajjakul S, Prapaisilp P, Bangchokdee S. CT and MR features that can help to differentiate between focal chronic pancreatitis and pancreatic cancer. Radiol Med 2020; 125; 356-364.

80) Izzo F, Granata V, Fusco R, D'Alessio V, Petrillo A, Lastoria S, Piccirillo M, Albino V, Belli A, Tafuto S, Avallone A, Patrone R, Palaia R. Clinical Phase I/II Study: Local Disease Control and Survival in Locally

Advanced Pancreatic Cancer Treated with Electrochemotherapy. J Clin Med 2021; 10: 1305.

81) Gabelloni M, Di Nasso M, Morganti R, Faggioni L, Masi G, Falcone A, Neri E. Application of the ESR iGuide clinical decision support system to the imaging pathway of patients with hepatocellular carcinoma and cholangiocarcinoma: preliminary findings. Radiol Med 2020; 125, 531-537.

82) Granata V, Fusco R, Sansone M, Grassi R, Maio F, Palaia R, Tatangelo F, Botti G, Grimm R, Curley S, Avallone A, Izzo F, Petrillo A. Magnetic resonance imaging in the assessment of pancreatic cancer with quantitative parameter extraction by means of dynamic contrast-enhanced magnetic resonance imaging, diffusion kurtosis imaging and intravoxel incoherent motion diffusion-weighted imaging. Therap Adv Gastroenterol 2020; 13: 1756284819885052.

83) Cholangiocarcinoma Working Group. Italian Clinical Practice Guidelines on Cholangiocarcinoma - Part I: Classification, diagnosis and staging. Dig Liver Dis 2020; 52: 1282-1293.

84) Cholangiocarcinoma Working Group. Italian Clinical Practice Guidelines on Cholangiocarcinoma - Part II: Treatment. Dig Liver Dis 2020; 52: 1430-1442.

85) Blay JY, Casali P, Bouvier C, Dehais C, Galloway I, Gietema J, Halámková J, Hindi N, Idbaih A, Kinloch E, Klümpen HJ, Kolarova T, Kopeckova K, Lovey J, Magalhaes M, Oselin K, Piperno-Neumann S, Ravnsbaek A, Rogasik M, Safwat A, Scheipl S, Seckl M, Taylor J, Temnyk M, Trama A, Urbonas M, Wartenberg M, Weinman A; EURACAN Network. European Reference Network for rare adult solid cancers, statement and integration to health care systems of member states: a position paper of the ERN EURACAN. ESMO Open 2021; 6: 100174.

86) Barrak D, Desale S, Yoon JJ, Dugan MM, Kodavanti PP, Sampah ME, Sugarbaker PH. Appendiceal tumors with glandular and neuroendocrine features exhibiting peritoneal metastases - Critical evaluation of outcome following cytoreductive surgery with perioperative chemotherapy. Eur J Surg Oncol 2021; 47: 1278-1285.

87) Granata V, Fusco R, Setola SV, Castelguidone ELD, Camera L, Tafuto S, Avallone A, Belli A, Incollingo P, Palaia R, Izzo F, Petrillo A. The multidisciplinary team for gastroenteropancreatic neuroendocrine tumours: the radiologist's challenge. Radiol Oncol 2019; 53: 373-387.

88) Chiti G, Grazzini G, Cozzi D, Danti G, Matteuzzi B, Granata V, Pradella S, Recchia L, Brunese L, Miele V. Imaging of Pancreatic Neuroendocrine Neoplasms. Int J Environ Res Public Health 2021; 18: 8895.

89) Petralia G, Summers PE, Agostini A, Ambrosini R, Cianci R, Cristel G, Calistri L, Colagrande S. Dynamic contrast-enhanced MRI in oncology: how we do it. Radiol Med 2020; 125: 1288-1300.

90) Gregucci F, Fozza A, Falivene S, Smaniotto D, Morra A, Daidone A, Barbara R, Ciabattoni A; Italian Society of Radiotherapy and Clinical Oncology (AIRO) Breast Group. Present clinical practice of breast cancer radiotherapy in Italy: a nationwide survey by the Italian Society of Radiotherapy and Clinical Oncology (AIRO) Breast Group. Radiol Med 2020; 125: 674-682.

91) Kirienko M, Ninatti G, Cozzi L, Voulaz E, Gennaro N, Barajon I, Ricci F, Carlo-Stella C, Zucali P, Sollini M, Balzarini L, Chiti A. Computed tomography (CT)-derived radiomic features differentiate prevascular mediastinum masses as thymic neoplasms versus lymphomas. Radiol Med 2020; 125: 951-960.

92) Yılmaz BD, Uysal E, Gurdal N, Ozkan A. Is there any correlation between HPV and early radioresponse before brachytherapy in cervix uteri carcinoma? Radiol Med 2020; 125: 981-989.

93) Feng Y, Liu H, Ding Y, Zhang Y, Liao C, Jin Y, Ai C. Combined dynamic DCE-MRI and diffusion-weighted imaging to evaluate the effect of neoadjuvant chemotherapy in cervical cancer. Tumori 2020; 106: 155-164.

94) Berthelin MA, Barral M, Eveno C, Rousset P, Dautry R, Pocard M, Soyer P, Dohan A. Preoperative assessment of splenic involvement in patients with peritoneal carcinomatosis with CT and MR imaging. Eur J Radiol 2019; 110: 60-65.

95) Sun J, Yang L, Zhou Z, Zhang D, Han W, Zhang Q, Peng Y. Performance evaluation of two iterative reconstruction algorithms, MBIR and ASIR, in low radiation dose and low contrast dose abdominal CT in children. Radiol Med 2020; 125: 918-925.

96) Walkey MM, Friedman AC, Sohotra P, Radecki PD. CT manifestations of peritoneal carcinomatosis. AJR Am J Roentgenol 1988; 150: 1035-1041.

97) Cianci R, Delli Pizzi A, Patriarca G, Massari R, Basilico R, Gabrielli D, Filippone A. Magnetic Resonance Assessment of Peritoneal Carcinomatosis: Is There a True Benefit From Diffusion-Weighted Imaging? Curr Probl Diagn Radiol 2020; 49: 392-397.

98) Dresen RC, De Vuysere S, De Keyzer F, Van Cutsem E, Prenen H, Vanslembrouck R, De Hertogh G, Wolthuis A, D'Hoore A, Vandecaveye V. Whole-body diffusion-weighted MRI for operability assessment in patients with colorectal cancer and peritoneal metastases. Cancer Imaging 2019; 19: 1.

99) Dohan A, Hoeffel C, Soyer P, Jannot AS, Valette PJ, Thivolet A, Passot G, Glehen O, Rousset P. Evaluation of the peritoneal carcinomatosis index with CT and MRI. Br J Surg 2017; 104: 1244-1249.

100) Dong L, Li K, Peng T. Diagnostic value of diffusion-weighted imaging/magnetic resonance imaging for peritoneal metastasis from malignant tumor: A systematic review and meta-analysis. Medicine (Baltimore) 2021; 100: e24251.

101) Sammartino P, Biacchi D, Cornali T, Accarpio F, Sibio S, Luraschi B, Impagnatiello A, Di Giorgio A. Computerized System for Staging Peritoneal Surface Malignancies. Ann Surg Oncol 2016; 23: 1454-1460.

102) Zhang L, Kang L, Li G, Zhang X, Ren J, Shi Z, Li J, Yu S. Computed tomography-based radiomics model for discriminating the risk stratification of gastrointestinal stromal tumors. Radiol Med 2020; 125: 465-473.

103) Gurgitano M, Angileri SA, Rodà GM, Liguori A, Pandolfi M, Ierardi AM, Wood BJ, Carrafiello G. Interventional Radiology ex-machina: impact of Artificial Intelligence on practice. Radiol Med 2021; 126: 998-1006.

104) Barretta ML, Catalano O, Setola SV, Granata V, Marone U, D'Errico Gallipoli A. Gallbladder metastasis: spectrum of imaging findings. Abdom Imaging 2011; 36: 729-734.

105) Nakamura Y, Higaki T, Honda Y, Tatsugami F, Tani C, Fukumoto W, Narita K, Kondo S, Akagi M, Awai K. Advanced CT techniques for assessing hepatocellular carcinoma. Radiol Med 2021; 126: 925-935.

106) Sugarbaker PH. Peritoneal carcinomatosis: principle of management. Boston: Kluwer Academic; 1996.

107) Sugarbaker PH. Cytoreductive surgery and perioperative chemotherapy for peritoneal surface malignancy. Textbook and video atlas. Woodbury: Cine-Med Publishing Inc; 2013.

108) Chua TC, Moran BJ, Sugarbaker PH, Levine EA, Glehen O, Gilly FN, Baratti D, Deraco M, Elias D, Sardi A, Liauw W, Yan TD, Barrios P, Gómez Portilla A, de Hingh IH, Ceelen WP, Pelz JO, Piso P, González-Moreno S, Van Der Speeten K, Morris DL. Early- and long-term outcome data of patients with pseudomyxoma peritonei from appendiceal origin treated by a strategy of cytoreductive surgery and hyperthermic intraperitoneal chemotherapy. J Clin Oncol 2012; 30: 2449-2456.

109) Duhr CD, Kenn W, Kickuth R, Kerscher AG, Germer CT, Hahn D, Pelz JO. Optimizing of preoperative computed tomography for diagnosis in patients with peritoneal carcinomatosis. World J Surg Oncol 2011; 9: 171.

110) Di Giuliano F, Minosse S, Picchi E, Ferrazzoli V, Da Ros V, Muto M, Pistolese CA, Garaci F, Floris R. Qualitative and quantitative analysis of 3D T1 Silent imaging. Radiol Med 2021; 126: 1207-1215.

111) Scapicchio C, Gabelloni M, Barucci A, Cioni D, Saba L, Neri E. A deep look into radiomics. Radiol Med 2021; 126: 1296-1311.

112) Agarwal M, van der Pol CB, Patlas MN, Udare A, Chung AD, Rubino J. Optimizing the radiologist work environment: Actionable tips to improve workplace satisfaction, efficiency, and minimize burnout. Radiol Med 2021; 126: 1255-1257.

113) Karmazanovsky G, Gruzdev I, Tikhonova V, Kondratyev E, Revishvili A. Computed tomography-based radiomics approach in pancreatic tumors characterization. Radiol Med 2021. doi: 10.1007/s11547-021-01405-0. Online ahead of print.

114) Qin H, Que Q, Lin P, Li X, Wang XR, He Y, Chen JQ, Yang H. Magnetic resonance imaging (MRI) radiomics of papillary thyroid cancer (PTC): a comparison of predictive performance of multiple classifiers modeling to identify cervical lymph node metastases before surgery. Radiol Med 2021; 126: 1312-1327.

115) Polk SL, Choi JW, McGettigan MJ, Rose T, Ahmed A, Kim J, Jiang K, Balagurunathan Y, Qi J, Farah PT, Rathi A, Permuth JB, Jeong D. Multiphase computed tomography radiomics of pancreatic intraductal papillary mucinous neoplasms to predict malignancy. World J Gastroenterol 2020; 26: 3458-3471.

116) Satake H, Ishigaki S, Ito R, Naganawa S. Radiomics in breast MRI: current progress toward clinical application in the era of artificial intelligence. Radiol Med 2022; 127: 39-56.

117) Song XL, Ren JL, Yao TY, Zhao D, Niu J. Radiomics based on multisequence magnetic resonance imaging for the preoperative prediction of peritoneal metastasis in ovarian cancer. Eur Radiol 2021; 31: 8438-8446.

118) Dong D, Tang L, Li ZY, Fang MJ, Gao JB, Shan XH, Ying XJ, Sun YS, Fu J, Wang XX, Li LM, Li ZH, Zhang DF, Zhang Y, Li ZM, Shan F, Bu ZD, Tian J, Ji JF. Development and validation of an individualized nomogram to identify occult peritoneal metastasis in patients with advanced gastric cancer. Ann Oncol 2019; 30: 431-438.

119) Liu S, He J, Liu S, Ji C, Guan W, Chen L, Guan Y, Yang X, Zhou Z. Radiomics analysis using contrast-enhanced CT for preoperative prediction of occult peritoneal metastasis in advanced gastric cancer. Eur Radiol 2020; 30: 239-246.

120) Crimì F, Capelli G, Spolverato G, Bao QR, Florio A, Milite Rossi S, Cecchin D, Albertoni L, Campi C, Pucciarelli S, Stramare R. MRI T2-weighted sequences-based texture analysis (TA) as a predictor of response to neoadjuvant chemo-radiotherapy (nCRT) in patients with locally advanced rectal cancer (LARC). Radiol Med 2020; 125: 1216-1224.

121) Fusco R, Grassi R, Granata V, Setola SV, Grassi F, Cozzi D, Pecori B, Izzo F, Petrillo A. Artificial Intelligence and COVID-19 Using Chest CT Scan and Chest X-ray Images: Machine Learning and Deep Learning Approaches for Diagnosis and Treatment. J Pers Med 2021; 11: 993.

122) Sansone M, Grassi R, Belfiore MP, Gatta G, Grassi F, Pinto F, La Casella GV, Fusco R, Cappabianca S, Granata V, Grassi R. Radiomic features of breast parenchyma: assessing differences between FOR PROCESSING and FOR PRESENTATION digital mammography. Insights Imaging 2021; 12: 147.

123) Granata V, Fusco R, Costa M, Picone C, Cozzi D, Moroni C, La Casella GV, Montanino A, Monti R, Mazzoni F, Grassi R, Malagnino VG, Cappabianca S, Grassi R, Miele V, Petrillo A. Preliminary Report on Computed Tomography Radiomics Features as Biomarkers to Immunotherapy Selection in Lung Adenocarcinoma Patients. Cancers (Basel) 2021; 13: 3992.

124) Granata V, Grassi R, Fusco R, Belli A, Cutolo C, Pradella S, Grazzini G, La Porta M, Brunese MC, De Muzio F, Ottaiano A, Avallone A, Izzo F, Petrillo A. Diagnostic evaluation and ablation treatments assessment in hepatocellular carcinoma. Infect Agent Cancer 2021; 16: 53.

125) Granata V, Fusco R, Barretta ML, Picone C, Avallone A, Belli A, Patrone R, Ferrante M, Cozzi D,

Grassi R, Grassi R, Izzo F, Petrillo A. Radiomics in hepatic metastasis by colorectal cancer. Infect Agent Cancer 2021; 16: 39.

126) Fusco R, Piccirillo A, Sansone M, Granata V, Rubulotta MR, Petrosino T, Barretta ML, Vallone P, Di Giacomo R, Esposito E, Di Bonito M, Petrillo A. Radiomics and Artificial Intelligence Analysis with Textural Metrics Extracted by Contrast-Enhanced Mammography in the Breast Lesions Classification. Diagnostics (Basel) 2021; 11: 815.

127) Fusco R, Granata V, Mazzei MA, Meglio ND, Roscio DD, Moroni C, Monti R, Cappabianca C, Picone C, Neri E, Coppola F, Montanino A, Grassi R, Petrillo A, Miele V. Quantitative imaging decision support (QIDS™) tool consistency evaluation and radiomic analysis by means of 594 metrics in lung carcinoma on chest CT scan. Cancer Control 2021; 28: 1073274820985786.

128) Fusco R, Granata V, Petrillo A. Introduction to Special Issue of Radiology and Imaging of Cancer. Cancers (Basel) 2020; 12: 2665.

129) Danti G, Berti V, Abenavoli E, Briganti V, Linguanti F, Mungai F, Pradella S, Miele V. Diagnostic imaging of typical lung carcinoids: relationship between MDCT, (111)In-Octreoscan and (18)F-FDG-PET imaging features with Ki-67 index. Radiol Med 2020; 125, 715-729.

130) Esposito A, Buscarino V, Raciti D, Casiraghi E, Manini M, Biondetti P, Forzenigo L. Characterization of liver nodules in patients with chronic liver disease by MRI: performance of the Liver Imaging Reporting and Data System (LI-RADS v.2018) scale and its comparison with the Likert scale. Radiol Med 2020; 125, 15-23.

131) Farchione A, Larici AR, Masciocchi C, Cicchetti G, Congedo MT, Franchi P, Gatta R, Lo Cicero S, Valentini V, Bonomo L, Manfredi R. Exploring technical issues in personalized medicine: NSCLC survival prediction by quantitative image analysis-usefulness of density correction of volumetric CT data. Radiol Med 2020; 125: 625-635.

132) Fornell-Perez R, Vivas-Escalona V, Aranda-Sanchez J, Gonzalez-Dominguez MC, Rubio-Garcia J, Aleman-Flores P, Lozano-Rodriguez A, Porcel-de-Peralta G, Loro-Ferrer JF. Primary and post-chemoradiotherapy MRI detection of extramural venous invasion in rectal cancer: the role of diffusion-weighted imaging. Radiol Med 2020; 125: 522-530.

133) Gündoğdu E, Emekli E, Kebapçı M. Evaluation of relationships between the final Gleason score, PI-RADS v2 score, ADC value, PSA level, and tumor diameter in patients that underwent radical prostatectomy due to prostate cancer. Radiol Med 2020; 125, 827-837.

134) Granata V, Fusco R, Amato DM, Albino V, Patrone R, Izzo F, Petrillo A. Beyond the vascular profile: conventional DWI, IVIM and kurtosis in the assessment of hepatocellular carcinoma. Eur Rev Med Pharmacol Sci 2020; 24: 7284-7293.

135) Fusco R, Raiano N, Raiano C, Maio F, Vallone P, Mattace Raso M, Setola SV, Granata V, Rubulotta MR, Barretta ML, Petrosino T, Petrillo A. Evaluation of average glandular dose and investigation of the relationship with compressed breast thickness in dual energy contrast enhanced digital mammography and digital breast tomosynthesis. Eur J Radiol 2020; 126: 108912.

136) Fusco R, Granata V, Maio F, Sansone M, Petrillo A. Textural radiomic features and time-intensity curve data analysis by dynamic contrast-enhanced MRI for early prediction of breast cancer therapy response: preliminary data. Eur Radiol Exp 2020; 4: 8.

137) Hu HT, Shan QY, Chen SL, Li B, Feng ST, Xu EJ, Li X, Long JY, Xie XY, Lu MD, Kuang M, Shen JX, Wang W. CT-based radiomics for preoperative prediction of early recurrent hepatocellular carcinoma: technical reproducibility of acquisition and scanners. Radiol Med 2020; 125: 697-705.

138) Lian S, Zhang C, Chi J, Huang Y, Shi F, Xie C. Differentiation between nasopharyngeal carcinoma and lymphoma at the primary site using whole-tumor histogram analysis of apparent diffusion coefficient maps. Radiol Med 2020; 125: 647-653.

139) Minutoli F, Pergolizzi S, Blandino A, Mormina E, Amato E, Gaeta M. Effect of granulocyte colony-stimulating factor on bone marrow: evaluation by intravoxel incoherent motion and dynamic contrast-enhanced magnetic resonance imaging. Radiol Med 2020; 125: 280-287.

140) Nazari M, Shiri I, Hajianfar G, Oveisi N, Abdollahi H, Deevband MR, Oveisi M, Zaidi H. Noninvasive Fuhrman grading of clear cell renal cell carcinoma using computed tomography radiomic features and machine learning. Radiol Med 2020; 125: 754-762.

141) Neri E, Coppola F, Miele V, Bibbolino C, Grassi R. Artificial intelligence: Who is responsible for the diagnosis? Radiol Med 2020; 125: 517-521.

142) Neri E, Miele V, Coppola F, Grassi R. Use of CT and artificial intelligence in suspected or COVID-19 positive patients: statement of the Italian Society of Medical and Interventional Radiology. Radiol Med 2020; 125: 505-508.

143) Benedetti G, Mori M, Panzeri MM, Barbera M, Palumbo D, Sini C, Muffatti F, Andreasi V, Steidler S, Doglioni C, Partelli S, Manzoni M, Falconi M, Fiorino C, De Cobelli F. CT-derived radiomic features to discriminate histologic characteristics of pancreatic neuroendocrine tumors. Radiol Med 2021; 126: 745-776.

144) Agazzi GM, Ravanelli M, Roca E, Medicina D, Balzarini P, Pessina C, Vermi W, Berruti A, Maroldi R, Farina D. CT texture analysis for prediction of EGFR mutational status and ALK rearrangement in patients with non-small cell lung cancer. Radiol Med 2021; 126: 745-760.

145) Santone A, Brunese MC, Donnarumma F, Guerriero P, Mercaldo F, Reginelli A, Miele V, Giovagnoni A, Brunese L. Radiomic features for prostate cancer grade detection through formal verification. Radiol Med 2021; 126: 688-697.

146) Cusumano D, Meijer G, Lenkowicz J, Chiloiro G, Boldrini L, Masciocchi C, Dinapoli N, Gatta R,

Casà C, Damiani A, Barbaro B, Gambacorta MA, Azario L, De Spirito M, Intven M, Valentini V. A field strength independent MR radiomics model to predict pathological complete response in locally advanced rectal cancer. Radiol Med 2021; 126: 421-429.

147) Paoletti M, Muzic SI, Marchetti F, Farina LM, Bastianello S, Pichiecchio A. Differential imaging of atypical demyelinating lesions of the central nervous system. Radiol Med 2021; 126: 827-842.

148) Sollazzo F, Liquori G, Di Nitto M, Failla A, De Leo A, D'Inzeo V, Chiappetta L, Amodei G, Messina C, Forte D, Montesano M, De Nuzzo D, Di Muzio M, Di Simone E, Dionisi S, Orsi GB, Giannetta N. Management and treatment of taste and smell alterations in oncologic patients undergoing antitumoral therapy and radiotherapy. WCRJ 2021; 8: e2123.

149) Rehab FM, Saad E. Challenges of patients with a rare combination of multiple primary malignancies: a single-center experience and a case series study. WCRJ 2021; 8: e2129.

150) Liang BQ, Zhou SG, Liu JH, Huang YM, Zhu X. Clinicopathologic features and outcome of cervical cancer: implications for treatment. Eur Rev Med Pharmacol Sci 2021; 25: 696-709.

151) Jayakrishnan T, Abel S, Reichstein A, Fortunato R, Nosik S, McCormick J, Finley G, Monga D, Kirichenko AV, Wegner RE. Retrospective analysis of the predictors of outcome following local excision for T1 rectal adenocarcinoma. WCRJ 2021; 8: e2094.

152) Kaplan E, Kaplan S. Author Correction: Computed tomographic perfusion imaging for the prediction of response transarterial radioembolization with Yttrium-90 glass microspheres of hepatocellular carcinoma. Eur Rev Med Pharmacol Sci 2021; 25: 6828.

153) Liao JH, Qin Q. Identification of ATXN3 and UBE2S as prognostic markers for osteosarcoma by a regression model for integrating multiomics. WCRJ 2021; 8: e2051.

154) Cong L, Hua QQ, Huang ZQ, Ma QL, Wang XM, Huang CC, Xu JX, Ma T. A radiomics method based on MR FS-T2WI sequence for diagnosing of autosomal dominant polycystic kidney disease progression. Eur Rev Med Pharmacol Sci 2021; 25: 5769-5780.

155) Granata V, Grassi R, Fusco R, Izzo F, Brunese L, Delrio P, Avallone A, Pecori B, Petrillo A. Current status on response to treatment in locally advanced rectal cancer: what the radiologist should know. Eur Rev Med Pharmacol Sci 2020; 24: 12050-12062.

156) Galmarini CM, Lucius M. Artificial intelligence: a disruptive tool for a smarter medicine. Eur Rev Med Pharmacol Sci 2020; 24: 7462-7474.

157) Homaei Shandiz F, Fekri F, Ghaffarzadegan K, Elyasi S, Bazrgari F, Niazi Moghadam MR, Hooshang Mohammadpour A. Human serum fatty acid binding protein as a prognostic factor in non-metastatic breast cancer patients: disappointing findings. WCRJ 2021; 8: e2047.